Biochemical characterization and subcellular localization of human copper transporter 1 (hCTR1)

Adriana E. M. KLOMP, Bastiaan B. J. TOPS, Inge E. T. VAN DEN BERG, Ruud BERGER and Leo W. J. KLOMP[1]

Department of Metabolic Diseases, University Medical Center Utrecht, Lundlaan 6, 3584 EA Utrecht, The Netherlands

The human copper transporter 1 gene (*hCTR1*) was previously identified by functional complementation in *ctr1*-deficient yeast. Overexpression of hCTR1 in wild-type yeast leads to increased sensitivity to copper toxicity, and mice with a homozygous disruption at the *Ctr1* locus die early during embryogenesis. It is proposed that hCTR1 is responsible for high-affinity copper uptake into human cells, but the underlying molecular mechanisms are unknown. To begin to investigate the biochemical characteristics of hCTR1, a polyclonal antiserum was raised against recombinant hCTR1-fusion peptides. Biosynthetic studies using this antiserum revealed that hCTR1 was synthesized as a precursor protein of 28 kDa containing N-linked oligosaccharides, and is then converted to a mature protein of approx. 35 kDa, which is ubiquitously expressed. Immunofluorescence studies showed that subcellular hCTR1 localization differed markedly between cell types. In some cell lines, hCTR1 was located predominantly in an intracellular vesicular perinuclear compartment, and in others hCTR1 was located predominantly at the plasma membrane. In contrast with the copper export P-type ATPases mutated in Wilson disease and Menkes disease, the localization of hCTR1 was not influenced by copper concentrations. Inhibition of endocytosis by methyl-β-cyclodextrin caused a partial redistribution of hCTR1 to the cell surface of HeLa cells. Taken together, the results in this study suggest a cell-specific control of copper uptake, which involves subcellular localization of the hCTR1 protein.

Key words: cell surface exposure, copper transport, solute carrier, N-linked glycosylation, perinuclear compartment.

INTRODUCTION

The transition metal copper is an essential trace element required for a variety of cellular processes, such as oxidative metabolism, neurotransmitter synthesis, free radical detoxification, iron uptake and maturation of connective tissue [1,2]. At elevated levels, copper can be toxic to the cell. One mechanism of toxicity is believed to involve the metal-catalysed generation of hydroxyl radicals in the Fenton reaction [3,4]. To balance the beneficial and toxic effects of this essential ion, all organisms possess homoeostatic mechanisms that properly control the cellular accumulation, distribution and detoxification of copper. The importance of maintaining the critical balance is underscored by the existence of two human genetic diseases in copper transport, Wilson disease and Menkes disease [5–10], which are characterized by copper accumulation and copper deficiency respectively.

Studies of cellular copper uptake in *Saccharomyces cerevisiae* have shown that copper is imported by two high-affinity copper-transport proteins, yCtr1p and yCtr3p [11,12]. Subsequently copper is carried to subcellular compartments or copper-dependent enzymes through the action of target-specific copper chaperone proteins that include Atx1 [13], yCCS [14] and yCox17 [15]. Consistent with the marked evolutionary conservation of the cellular mechanisms of copper homoeostasis, human orthologues of these copper chaperones have been characterized [14,16,17]. The human copper transporter 1 gene (*hCTR1*) was identified previously by functional complementation of the growth defect on non-fermentable medium of yeast cells defective in copper transport, due to inactivation of both the *yCTR1* and *yCTR3* genes [18]. hCTR1 is a 190-amino-acid protein with significant primary sequence similarity to yCtr1p and yCtr3p. The N-terminal domain of hCTR1 is rich in methionine and histidine residues, reminiscent of the methionine-rich N-terminal domain of yCtr1p, but it is much shorter than its yeast orthologue. Furthermore, like the *S. cerevisiae* Ctr1 and Ctr3 proteins, analysis of the membrane topology predicts the presence of three transmembrane domains. However, the topology of hCTR1 has not been experimentally addressed. Importantly, it was shown that mice with a homozygous disruption at the *mCtr1* locus have severe developmental defects and die *in utero*, presumably of copper deficiency [19,20]. Taken together with the ubiquitous expression of *mCtr1* during development [19,21], these findings suggest a crucial role for CTR1 in mammalian copper homoeostasis and embryonic development.

Despite the known essential role of CTR1, the molecular mechanisms of copper import into cells are not completely understood. It is proposed that like yCtr1p, hCTR1 is responsible for high-affinity copper uptake into human cells [18]. Immortalized cells transfected with cDNA constructs encoding hCTR1 and mCTR1 accumulate excess ^{64}Cu, suggesting that CTR1 represents the rate-limiting step in the delivery of copper to the cytosol [20,22], but it is unknown if CTR1 forms a plasma-membrane copper permease. In the present study, we have addressed the biochemical characteristics and the subcellular expression pattern of hCTR1 using a rabbit antiserum raised against a recombinant hCTR1-fusion peptide.

Abbreviations used: BFA, Brefeldin A; CTR1, copper transporter 1; Cy^{TM}3, indocarbocyanine; Endo H, endoglycosidase H; FAH, fumaryl acetoacetate hydrolase; FAH/6His, FAH tagged with six histidines residues; hCTR1, human CTR1; hCTR1-N/6His, N-terminus of hCTR1 tagged with six histidine residues; MβCD, methyl-β-cyclodextrin; p58, Golgi 58-kDa protein; TFR, transferrin receptor; TGN, *trans*-Golgi network; p230, TGN 230-kDa protein; VSV-G, vesicular-stomatitis-virus glycoprotein.

[1] To whom correspondence should be addressed (e-mail l.klomp@azu.nl).

EXPERIMENTAL

Cloning and expression of recombinant hCTR1

The region encoding the N-terminus of hCTR1 (amino acid residues 1–67) was amplified by PCR. We used the following specific oligonucleotides (Amersham Pharmacia Biotech, Little Chalfont, Bucks., U.K.) containing either a *Bam*HI (5′-CGG GAT CCG ATC ATT CCC ACC ATA TGG G-3′) or a *Sal*I (5′-CAG TCG ACT CCA GCT GTA TTG ATC ACC A-3′) restriction site (underlined) added to their 5′ ends. The PCR fragment was digested with *Bam*HI and *Sal*I, and was inserted into the prokaryotic expression vector pQE30 (Qiagen, Hilden, Germany) to generate a cDNA encoding the N-terminus of hCTR1 tagged with six histidine residues (hCTR1-N/6His). The correct open reading frame was confirmed by direct sequencing. The His_6-tagged fusion protein was purified from the transformed *Escherichia coli* strain M15(pREP4). The protein was dialysed against 0.1 M NaH_2PO_4/0.01 M Na_2CO_3, pH 5.0. Protein purity was ascertained by SDS/PAGE (12.5 % gel), followed by Coomassie Brilliant Blue staining. The recombinant full-length fumaryl acetoacetate hydrolase (FAH) protein tagged with six histidines residues (FAH/6His) was prepared in a similar manner (I.E.T. van den Berg and R. Berger, unpublished work).

Antiserum generation

Antiserum to hCTR1 was obtained by serial immunization of rabbits with the purified recombinant hCTR1-N/6His protein. Purified protein (250 μg) in an emulsion with Freund's adjuvant (Sigma, St. Louis, MO, U.S.A.) was injected subcutaneously. The crude antisera were affinity purified using hCTR1-N/6His coupled to CNBr-activated Sepharose™ 4B beads in accordance with the manufacturer's instructions (Sigma), and reconstituted in the original volume before utilization. In competition experiments, 10 μl of antiserum was incubated with 20–40 μg of purified antigen for 1 h at 4 °C.

Cloning of VSV-G tagged hCTR1

The full-length hCTR1 open reading frame was amplified by PCR using primers 5′-AAA ATG GAT CAT TCC CAC CAT-3′ and 5′-TCA CTT TCC TAG TCG GTT CAT CTC GAT GTC AGT GTA ATG GCA ATG CTC TGT GAT-3′. This resulted in a 3′ vesicular-stomatitis-virus glycoprotein (VSV-G)-tagged hCTR1 cDNA [23]. This cDNA was cloned into pZeoSV2 (Invitrogen, Carlsbad, CA, U.S.A.), and the correct sequence was confirmed by direct sequencing. VSV-G-tagged hCTR1 was synthesized *in vitro* with the TNT-coupled reticulocyte lysate system (Promega, Madison, WI, U.S.A.) according to the manufacturer's instructions, using the construct described above as template. Hybridoma clone P5D4 [anti-(VSV-G) antibody] was kindly provided by Dr J. Fransen (Department of Cell Biology, Nijmegen University, Nijmegen, The Netherlands).

Cell cultures

Cell lines were purchased from the A.T.C.C. (Rockville, MD, U.S.A.). Cells were cultured at 37 °C under humidified air containing 5 % CO_2, and according to the supplier's instructions. Culture media and solutions were purchased from Life Technologies (Breda, The Netherlands). For some experiments, cells were cultured in the presence of 400 μM $CuCl_2$ for 2 h or 50 μM bathocuproine disulphonic acid (Sigma) for 16 h in medium containing no fetal calf serum.

Nocodazole treatment was performed by incubating the cells in the presence of 20 mM nocodazole (Sigma) for 4 h at 37 °C in medium containing no fetal calf serum. The effect of Brefeldin A (BFA) was studied by incubating cells in the presence of 10 mg/ml BFA for 1–4 h at 37 °C (Epicentre Technologies, Madison, WI, U.S.A.). Endocytosis was inhibited by culturing the cells in the presence of 10 mM methyl-β-cyclodextrin (MβCD; Sigma) for 1 h at 37 °C in minimal essential medium-α supplemented with 20 mM Hepes, pH7.4, and 0.1 % BSA. Transient transfections were performed by electroporating 2.5×10^6 cells with 3 μg of purified plasmid DNA at 400 V and 250 μF using Gene Pulser II (Bio-Rad Laboratories BV, Veenendaal, The Netherlands).

Biosynthetic labelling of cell lines and immunoprecipitation

Cells were maintained at confluence, incubated in medium containing no methionine for 30 min, and subsequently metabolically labelled with 100 μCi/ml Tran[^{35}S]™ (specific activity > 1000 Ci/mmol; ICN Biomedicals, Costa Mesa, CA, U.S.A.) for 10–120 min at 37 °C. Following labelling, cells were chased with medium containing 50 mM unlabelled methionine for different time periods. For tunicamycin treatment, cells were incubated with 10 μg/ml tunicamycin (Roche, Basel, Switzerland) 4 h prior to and during the metabolic labelling period. Cells were scraped into lysis buffer (0.5 % Triton X-100, 150 mM NaCl, 10 mM sodium EDTA, 0.5 % sodium deoxycholic acid, 1 mM PMSF and 20 mM Tris/HCl, pH 7.4). Cell lysates were clarified by centrifugation at 14000 ***g*** for 30 min at 4 °C. hCTR1 was immunoprecipitated from the supernatants using 10 μl of affinity-purified rabbit anti-human hCTR1 antiserum pre-incubated for 2 h with 15 μl of Protein A agarose beads (Sigma), and 2 vol. buffer A (1 % SDS, 1 % Triton X-100, 0.5 % sodium deoxycholic acid, 0.5 % BSA and 1 mM PMSF, in PBS). The reactions were incubated overnight at 4 °C on a rotating wheel. Immunocomplexes were precipitated by microcentrifuge at 14000 ***g*** and washed five times with buffer A. All immunoprecipitates were resuspended in Laemmli buffer and heated at 95 °C for 5 min prior to SDS/PAGE (12.5 % gel) [24]. Gels were soaked in Amplify (Amersham Pharmacia Biotech) prior to fluorographic exposure.

For endoglycosidase H (Endo H) experiments, protein immunocomplexes were disrupted in 1 % SDS/1 % β-mercaptoethanol and treated with Endo H (Roche, Basel, Switzerland), according to the manufacturer's instructions.

Extract preparation, immunoprecipitation and Western-blot analysis

For the preparation of total cell extracts, monolayer cultures were harvested in cold lysis buffer. The extracts were clarified by centrifugation at 14000 ***g*** at 4 °C for 30 min, and the protein concentrations of the supernatants were determined by the Bio-Rad protein assay (Hercules, CA, U.S.A.), according to the manufacturer's instructions. For detection of steady-state hCTR1 expression, 10 μl of affinity-purified polyclonal anti-hCTR1 antiserum was pre-incubated with 15 μl of Protein A-agarose beads (Sigma), as described above. Cell extracts (1 mg of protein) were added, and hCTR1 was recovered by centrifugation. The immunocomplexes were resolved on SDS/PAGE and transferred to Hybond-P membranes (Amersham Pharmacia Biotech) by electrophoretic transfer in a Bio-Rad transblot cell using 20 % methanol, 0.15 M glycine, 0.025 % SDS and 0.02 M Tris-HCl, pH 7, as transfer buffer. Subsequently, the membranes were blocked in 5 % non-fat dried milk (Protifar; Nutricia, Zoetermeer, The Netherlands) in PBS and 0.05 % Tween-20. The immunoblots were probed with 1:1000 affinity purified anti-

hCTR1 antibody in 5% non-fat dried milk in PBS and 0.05% Tween-20 at 22 °C. Reactivity was detected with horseradish peroxidase-conjugated secondary antibodies (1:10000) and chemiluminescence (ECL™plus; Amersham Pharmacia Biotech), according to the manufacturer's instructions.

Confocal immunofluorescence microscopy

For fluorescence microscopy, cells were seeded and grown on cover slips (Marienfeld, Paul GmbH & Co.KG, Bad Mergentheim, Germany). After 36 h, cells were washed with PBS and fixed with 4% paraformaldehyde in PBS for 20 min at 4 °C. The cells were then washed three times with buffer B (PBS containing 0.02% Triton X-100) and blocked for 30 min with 5% BSA in buffer B at 22 °C. hCTR1 was stained with anti-hCTR1 antiserum (diluted 1:1000). ATP7A protein was stained as described previously [25], using antiserum kindly provided by Dr J. D. Gitlin (Edward Mallinckrodt Department of Pediatrics, Washington University School of Medicine, St. Louis, U.S.A.). For the double-labelling experiments monoclonal antibodies against Golgi 58-kDa protein (p58; diluted 1:50; Sigma), *trans*-Golgi network (TGN) 230-kDa protein (p230) (diluted 1:200; BD Biosciences, San Jose, CA, U.S.A.) and human transferrin receptor (TFR) (diluted 1:200; Molecular Probes, Eugene, OR, U.S.A.) were used. Antibodies were visualized by using indocarbocyanine (Cy™3)- or FITC-conjugated affiniPure donkey anti-mouse or anti-rabbit IgG (H + L) antibodies, diluted 1:2000 (Jackson ImmunoResearch Laboratories, West Grove, PA, U.S.A.). Lysosomes were stained by incubating cells for 1 h with 25 nM LysoTracker® (Molecular Probes) at 37 °C. The cover slips were mounted in Imsolmount (Klinipath, Duiven, The Netherlands), and confocal light microscopy analysis was performed on a laser scanning microscope (Leica TCS 4D) using dedicated image software.

RESULTS

Characterization of hCTR1 antiserum

The *hCTR1* gene encodes a protein containing three putative transmembrane domains, and a number of putative glycosylation sites. For the investigation of the biochemical characterization and subcellular localization of hCTR1, polyclonal antibodies were generated by immunizing rabbits with a 15-kDa recombinant protein, encoding the N-terminal part of hCTR1 tagged with six histidine residues (hCTR1-N/6His). To investigate whether the produced antiserum specifically detected hCTR1, immunoblot analysis was performed. From Figure 1(A), we conclude that the antiserum contained some antibodies that bound to the His_6 tag, but particularly contained antibodies that specifically recognized the N-terminal part of hCTR1. In this experiment and all subsequent experiments described below, immunoreactivity was completely absent when pre-immune serum was used. In addition, immunoreactivity was completely abolished by pre-incubation of anti-hCTR1 antibody with hCTR1-N/6His, but not by pre-incubation with an irrelevant His_6-tagged fusion protein (FAH/6His; Figure 1E and results not shown). Taken together, these results strongly suggest that the anti-hCTR1 antiserum utilized in the present study specifically recognized the hCTR1 protein.

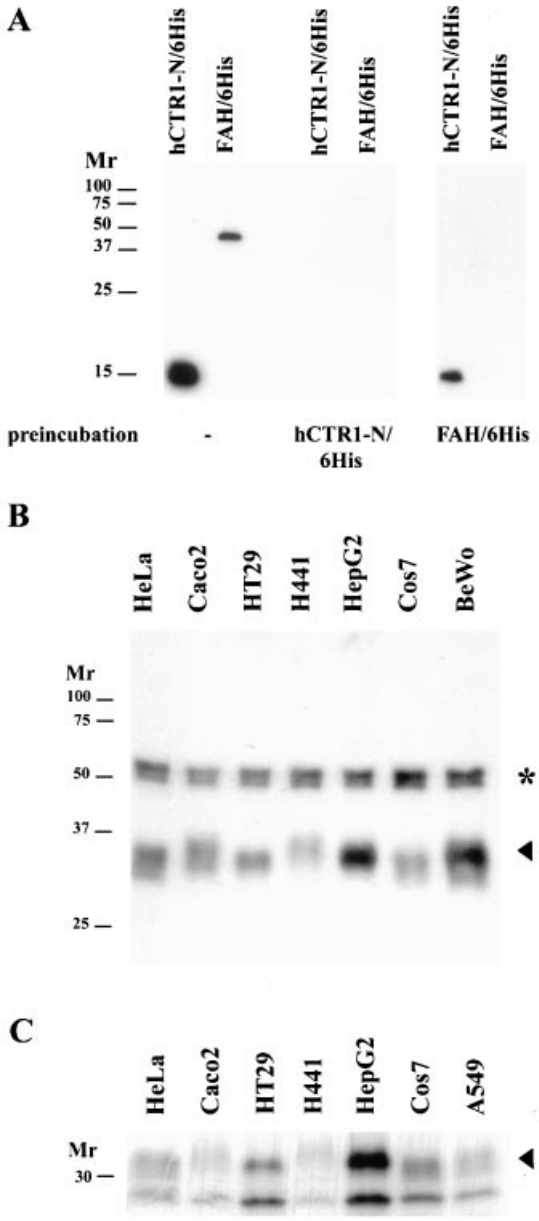

Figure 1 Characterization of anti-hCTR1 antiserum and expression of hCTR1 in different cell lines

(**A**) Immunoblot analysis of hCTR-N/6His and FAH/6His. Recombinant proteins (100 ng) were separated by SDS/PAGE, and transferred to nitrocellulose. Proteins were visualized with anti-hCTR1 antibody (left-hand lanes), anti-hCTR1 antibody pre-incubated with hCTR1-N/6His (middle lanes) or anti-hCTR1 antibody pre-incubated with FAH/6His (right-hand lanes), all followed by goat anti-rabbit peroxidase-conjugated antibody. (**B** and **C**) hCTR1 expression in different cell lines. (**B**) Cell lysates from different cell lines were prepared and hCTR1 was immunoprecipitated with anti-hCTR1 antibody, separated by SDS/PAGE, transferred to nitrocellulose and visualized with anti-hCTR1 antibody, followed by goat anti-rabbit peroxidase-conjugated antibody. The asterisk indicates the position of the immunoglobulin heavy chains from the immunoprecipitating antibodies. The arrowhead indicates the position of the 35-kDa protein. (**C**) Cells were labelled with Tran[^{35}S]^{TM} for 2 h and immunoprecipitation was performed with anti-hCTR1 antibody. Proteins were separated by SDS/PAGE, followed by fluorography.

Biochemical characterization of hCTR1 protein in different cell lines

To study the steady-state expression of hCTR1 in different cell lines, cells were lysed and used for immunoprecipitation with anti-hCTR1 antibody. After separation of immunoprecipitated proteins by SDS/PAGE and immunoblotting with anti-hCTR1 antibody, several proteins with the approximate molecular mass of 35 kDa, which appeared as heterogeneous smears on SDS/

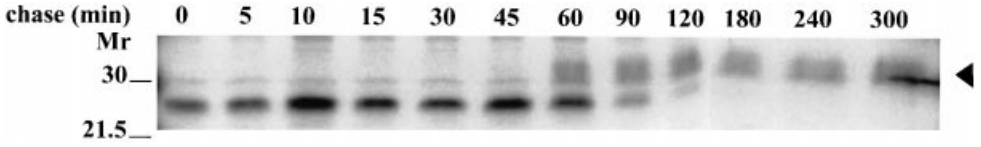

Figure 2 Pulse-chase analysis of hCTR1 biosynthesis

HeLa cells were pulse-labelled with Tran[^{35}S]^{TM} for 10 min and chased for the indicated time periods with cold methionine. Immunoprecipitation was performed with anti-hCTR1 antibody, and proteins were separated by SDS-PAGE, followed by fluorography. The arrowhead indicates the position of the 35-kDa protein.

PAGE, were detected (Figure 1B). The apparent molecular masses of these proteins differed between the investigated cell lines. To characterize newly synthesized hCTR1, cells were labelled for 2 h with Tran[^{35}S]^{TM}, lysed and used for immunoprecipitation with anti-hCTR1 antibody. As can be seen in Figure 1(C), in all cell lines proteins of approx. 35 kDa were detected, as shown similarly by immunoprecipitation of unlabelled hCTR1 (Figure 1B). Also, a protein with the apparent molecular mass of 28 kDa was detected in every cell line investigated.

Pulse-chase analysis of hCTR1

To investigate a possible relationship between the 28-kDa and the 35-kDa proteins, pulse-chase experiments were performed. HeLa cells were pulse-labelled with Tran[^{35}S]^{TM} for 10 min and subsequently chased for different time periods. Immunoprecipitation was performed with anti-hCTR1 antibody. Figure 2 shows that hCTR1 was synthesized initially as the polypeptide of 28 kDa and appeared as the protein of approx. 35 kDa after 60 min. Since the 28-kDa polypeptide gradually disappeared and was not detected after 3 h of chase, we concluded that the 28-kDa polypeptide is the precursor form of the 35-kDa protein. The 28-kDa polypeptide had a rapid turnover, whereas the half-life time of the 35-kDa mature protein was at least 2 days (results not shown). The same result was obtained when Cos7 or Caco2 cells were used (results not shown). The 28-kDa precursor polypeptide was not detected when hCTR1 was analysed under steady-state conditions (Figure 1B). This indicates that the steady-state concentration of this polypeptide was below the detection limit of the used method, which is probably due to the high turnover rate of the precursor when compared with the mature hCTR1 protein.

hCTR1 is a glycosylated protein

Based on the coding sequence of hCTR1, a protein backbone with a molecular mass of 23 kDa is predicted [18]. However, experiments described in the present study showed that anti-hCTR1 antibody specifically detected proteins with apparent molecular masses of 28 kDa and 35 kDa. The existence of several consensus N- and O-glycosylation sites in the amino acid sequence of hCTR1 raises the possibility that hCTR1 is a glycosylated protein *in vivo*. To test this hypothesis, HeLa cells were pre-incubated with tunicamycin, an inhibitor of N-glycosylation [26], for 4 h, followed by pulse-chase labelling in the presence of tunicamycin, and immunoprecipitation of hCTR1. As a result of tunicamycin treatment, hCTR1 was synthesized as a precursor with the apparent molecular mass of 23 kDa, which was converted to a 30-kDa polypeptide, clearly visible after 120 min (Figure 3A). No proteins with the apparent size of 35 kDa were formed in the presence of tunicamycin.

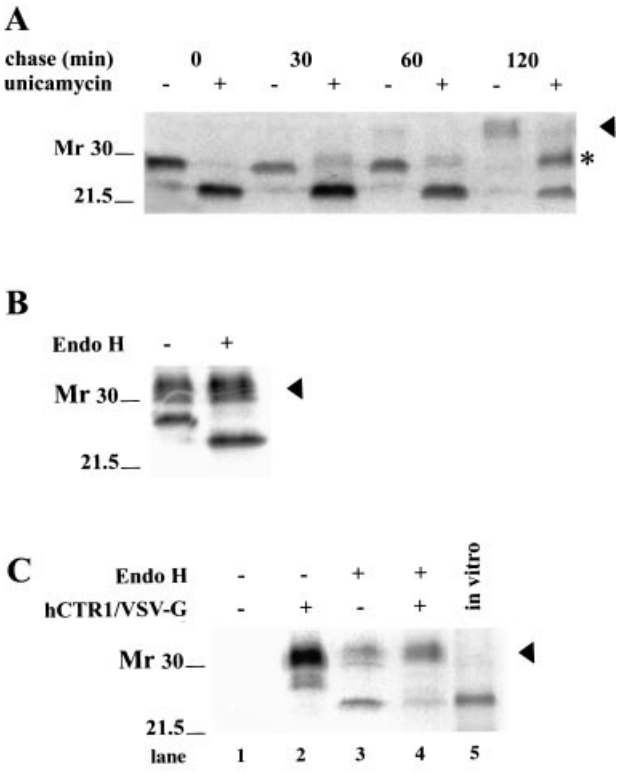

Figure 3 hCTR1 is a glycosylated protein

(**A**) HeLa cells were pre-incubated with or without tunicamycin for 4 h, and subsequently analysed as in Figure 2. (**B**) HeLa cells were labelled with Tran[^{35}S]^{TM} for 2 h and immunoprecipitation was performed with anti-hCTR1 antibody. After immunoprecipitation, proteins were treated with Endo H where indicated, separated by SDS/PAGE and analysed by fluorography. (**C**) Cos7 cells were transiently transfected with VSV-G-tagged hCTR1. Untransfected cells (lanes 1 and 3) and VSV-G-tagged hCTR1 transfected Cos7 cells (lanes 2 and 4) were labelled with Tran[^{35}S]^{TM} for 2 h and immunoprecipitation was performed with anti-(VSV-G) antibody (lanes 1, 2 and 4) or with anti-hCTR1 antibody (lane 3). Immunoprecipitates were treated with Endo H where indicated, separated by SDS/PAGE and analysed by fluorography. VSV-G-tagged hCTR1 was synthesized *in vitro* and analysed in lane 5. The arrowhead indicates the position of the 35-kDa protein; the asterisk indicates the position of the 30-kDa protein that is formed only in the presence of tunicamycin.

To further investigate the possibility of N-linked glycosylation of hCTR1, proteins immunoprecipitated by anti-hCTR1 antibody were treated with Endo H, an enzyme that removes high-mannose N-linked oligosaccharides from the protein backbone [27]. Upon incubation with Endo H, the 28-kDa protein was converted to a 23-kDa polypeptide. The 35-kDa protein was not sensitive to Endo-H treatment (Figure 3B).

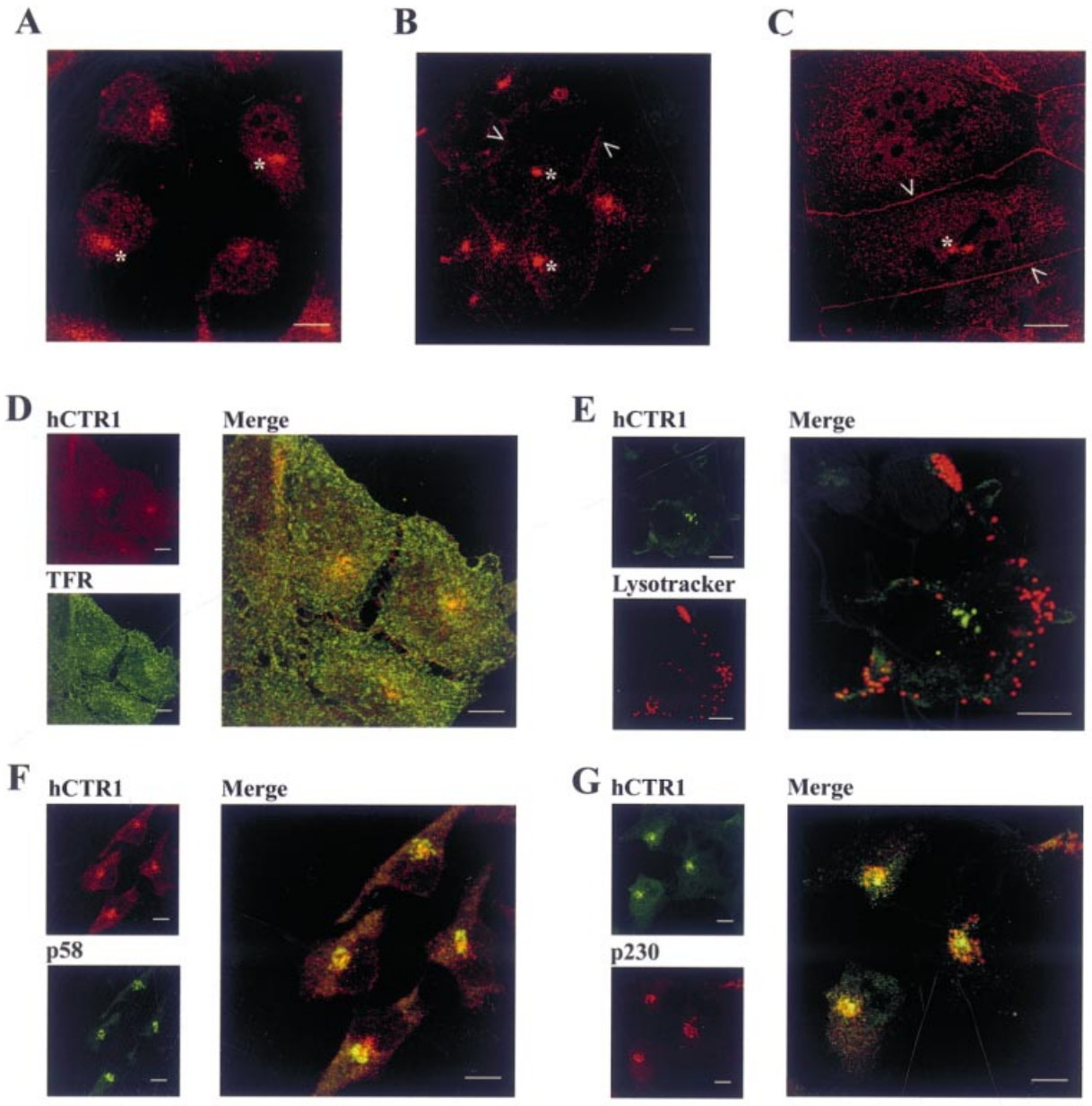

Figure 4 Subcellular localization of hCTR1 in different cell lines

HeLa cells (**A**), BeWo cells (**B**) or Caco2 cells (**C**) were analysed by indirect confocal immunofluorescence using anti-hCTR1 antibody followed by Cy^{TM}3-conjugated donkey anti-rabbit IgG antibody. Open arrowheads indicate plasma membranes, and asterisks indicate concentrated perinuclear immunostaining. (**D**) HeLa cells were analysed by double-label indirect immunofluorescence using anti-hCTR1 antibody visualized with Cy^{TM}3-conjugated donkey anti-rabbit IgG antibody, and anti-TFR antibody visualized with FITC-conjugated donkey anti-mouse IgG antibody. (**E**) HeLa cells were incubated for 1 h with LysoTracker®. hCTR1 was visualized with anti-hCTR1 antibody and FITC-conjugated donkey anti-rabbit IgG antibody. (**F**) Double labelling of hCTR1 and p58, visualized by Cy^{TM}3-conjugated donkey anti-rabbit IgG antibody and FITC-conjugated donkey anti-mouse IgG antibody respectively. (**G**) Double labelling of hCTR1 and p230, visualized by FITC-conjugated donkey anti-rabbit IgG antibody and Cy3-conjugated donkey anti-mouse IgG antibody respectively. Overlap in staining patterns is depicted in yellow in the merged images. The scale bars represent 10 μm.

An expression vector encoding VSV-G-tagged hCTR1 was constructed and used to transiently transfect Cos7 cells. Cells were metabolically labelled for 2 h with Tran[^{35}S]^{TM} 48 h after transfection, lysed and used for immunoprecipitation with anti-(VSV-G) antibody. In untransfected Cos7 cells, no proteins were detected with this antibody (Figure 3C, lane 1), whereas in cells transfected with pZeoSV2 encoding VSV-G epitope tagged hCTR1, proteins with apparent molecular masses of 28 kDa and 35 kDa were detected (Figure 3C, lane 2). This result indicates that exogenous VSV-G tagged hCTR1 and endogenous hCTR1 have similar electrophoretic mobilities, and that the C-terminal VSV-G tag does not affect the stability or the maturation of hCTR1. When immunoprecipitated exogenous VSV-G-tagged hCTR1 was treated with Endo H, a 35-kDa protein and a polypeptide with a molecular mass of 23 kDa (Figure 3C, lane 4) were detected, similar to Endo H treatment of immunoprecipitated endogenous hCTR1 (Figure 3C, lane 3). To investigate whether the 23-kDa protein band indeed represents the

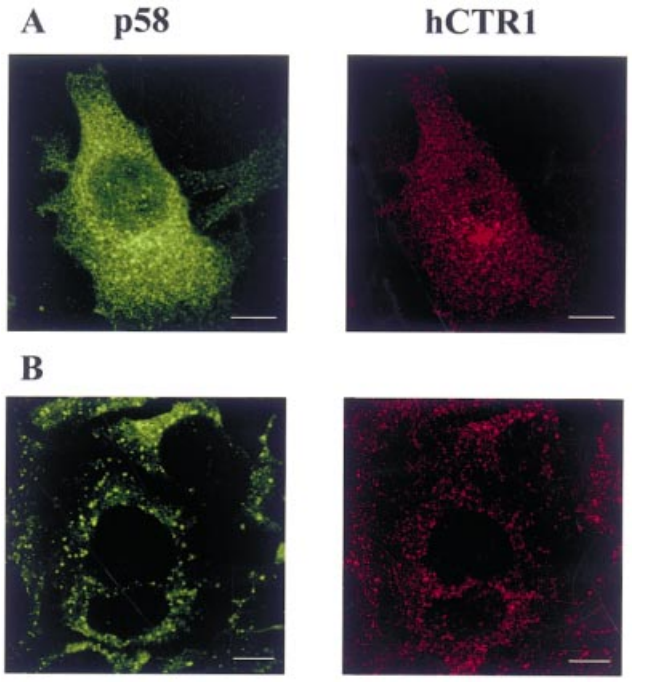

Figure 5 Effect of BFA and nocodazole on hCTR1 localization

(**A**) HeLa cells were treated with BFA and analysed by double-label indirect immunofluorescence of p58 and hCTR1, visualized by FITC-conjugated donkey anti-mouse IgG antibody and Cy™3-conjugated donkey anti-rabbit IgG antibody respectively. (**B**) HeLa cells were treated with nocodazole, and p58 and hCTR1 localization was analysed as in (**A**). The scale bars represent 10 μm.

hCTR1 protein backbone, VSV-G-tagged hCTR1 was synthesized *in vitro* in the absence of microsomes, thereby preventing glycosylation (Figure 3C, lane 5). The electrophoretic mobility of this polypeptide was identical with that of the polypeptide resulting from Endo-H treatment of immunoprecipitated hCTR1 (compare Figure 3C, lanes 4 and 5). Taken together, these results indicate that the 35-kDa protein detected by our antiserum is mature hCTR1. Furthermore, the biosynthesis of hCTR1 involves N-linked glycosylation and possibly O-linked glycosylation of a 28-kDa precursor polypeptide.

Subcellular localization of hCTR1 differs between cell lines

To investigate the subcellular localization of hCTR1, several cell lines were analysed by indirect immunofluorescence using anti-hCTR1 antibody. In the cervical carcinoma cell line HeLa, hCTR1 was located in a cytoplasmic vesicular compartment, concentrated around the nucleus (Figure 4A). No fluorescence was detected at the edges of the cells. Also in the lung carcinoma cell lines A549 and H441, and in the hepatocellular carcinoma cell line HepG2, hCTR1 was predominantly localized in a similar intracellular compartment (results not shown). In the choriocarcinoma placental cell line BeWo, hCTR1 was localized partially on the plasma membrane, but most prominently in an intracellular perinuclear compartment (Figure 4B). In the colon carcinoma cell lines Caco2 (Figure 4C) and HT29 (results not shown), hCTR1 was predominantly located at the plasma membrane, but vesicular intracellular staining was also clearly observed. The intracellular staining pattern in Caco2 cells appeared more diffusely localized compared with other cell types (Figure 4C).

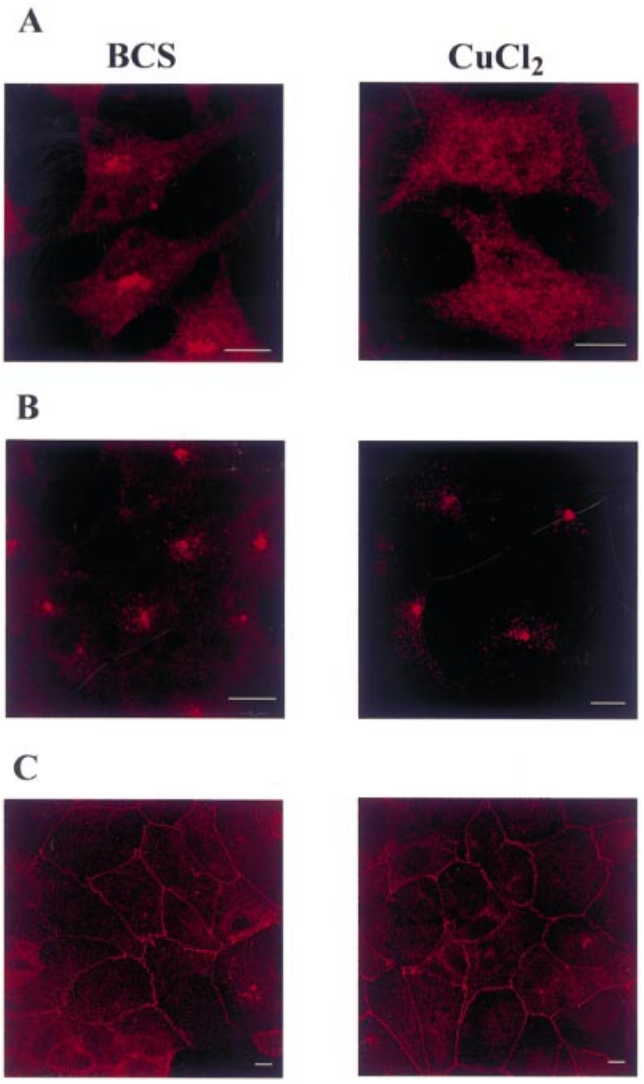

Figure 6 Effect of copper on hCTR1 localization

HeLa cells (**A** and **B**) or Caco 2 cells (**C**) were cultured in the presence of bathocuproine disulphonic acid (BCS) or 400 μM $CuCl_2$. Cells were fixed and stained for ATP7A (**A**), the protein mutated in Menkes disease, or for hCTR1 (**B** and **C**) as in Figure 4.The scale bars represent 10 μm.

The predominant intracellular localization in HeLa cells of hCTR1 is remarkable, since exogenous epitope-tagged yCtr1p is localized on the plasma membrane in yeast [28]. To further define the intracellular localization of hCTR1 in HeLa cells, double-labelling studies with different intracellular markers were performed. Areas of overlap in distribution, generated using computer-based superimposition by image processing, are shown in yellow (Figure 4). hCTR1 localization showed little to no overlap in distribution with the TFR protein, which is localized on the plasma membrane and in an early endosomal compartment (Figure 4D). Also no overlap with LysoTracker®, a marker for the lysosomes, was detected (Figure 4E). However, hCTR1 partially overlapped with the Golgi markers p58 and p230 (Figures 4F and 4G). Although intracellular hCTR1 staining in Caco2 cells appeared diffuse, hCTR1 immunoreactivity also overlapped partially with Golgi markers p58 and p230 in these cells (results not shown).

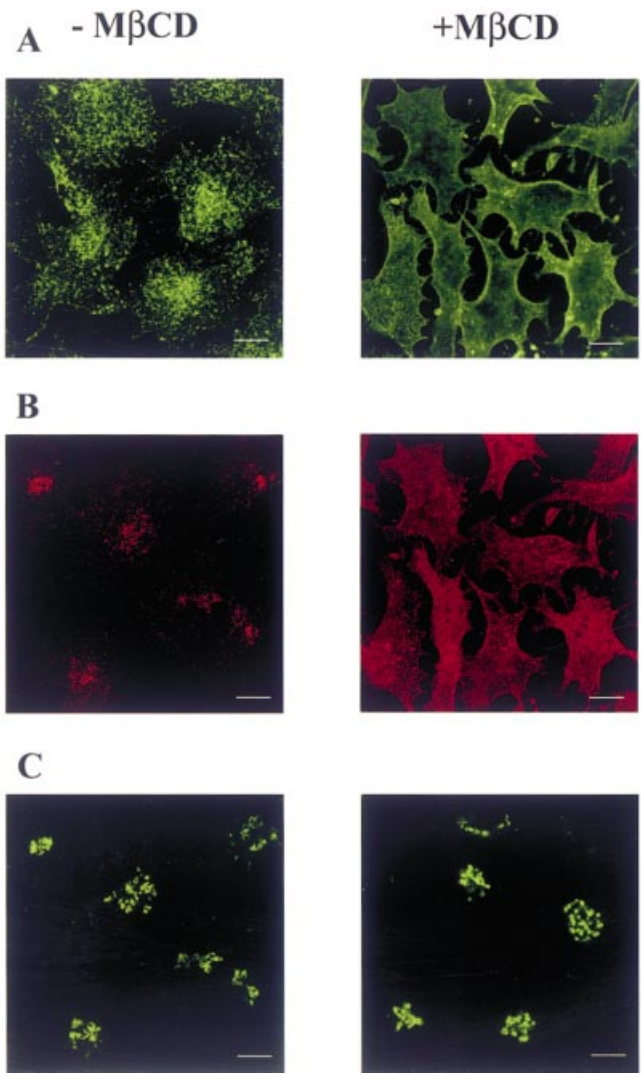

Figure 7 Effect of MβCD on hCTR1 localization

HeLa cells were cultured in the presence of MβCD, fixed and stained for TFR (**A**), hCTR1 (**B**) or p230 (**C**) as in Figure 4. The scale bars represent 10 μm.

The effects of two metabolites known to disrupt the Golgi compartment, namely BFA and nocodazole, on hCTR1 localization in HeLa cells were tested. BFA treatment resulted in redistribution of p58, but had no effect on hCTR1 localization (Figure 5A). In the presence of nocodazole, p58 no longer localized to identifiable Golgi structures, but scattered throughout the cytoplasm and patched to enlarged vesicles (Figure 5B). The perinuclear localization of hCTR1 was also dispersed as a result of nocodazole treatment.

hCTR1 localization is not influenced by extracellular copper concentrations

To investigate whether the localization of hCTR1 is responsive to extracellular copper concentrations, as described previously for the ATP7A and ATP7B proteins [29–32], HeLa and Caco2 cells were cultured in the presence of 50 μM bathocuproine disulphonic acid, a copper chelator, or 400 μM $CuCl_2$. Cells were fixed and stained for hCTR1 or ATP7A. ATP7A is a resident TGN protein, which redistributes upon copper addition, as was previously reported [25,29,31] (Figure 6A). In contrast, the localization of hCTR1 in HeLa and Caco2 cells is not influenced by extracellular copper concentrations under the conditions used (Figures 6B and 6C).

To test whether hCTR1 cycles through different compartments of the cell, HeLa cells were cultured in the presence of MβCD, an inhibitor of endocytosis via cholesterol depletion of the plasma membrane [33]. The subcellular localization of the TFR, a protein known to be endocytosed [34], changed upon MβCD treatment from the early endosomal compartment to a plasma-membrane localization (Figure 7A). In the absence of MβCD, no hCTR1 was detected on the plasma membrane of HeLa cells (Figure 7B). In the MβCD-treated cells, hCTR1 was not located in clearly well-defined intracellular structures, but redistributed to a vesicular compartment diffusely located in the cell. A significant fraction of the cellular hCTR1 was also located on the plasma membrane under the conditions used. The observed redistribution is not a result from fragmentation of the Golgi apparatus, since p230 localization is not altered (Figure 7C). These results suggest that steady-state localization of hCTR1 is the result of a dynamic process involving endocytosis from the cell surface.

DISCUSSION

Recently, it has been shown that mice with a homozygous disruption at the *Ctr1* locus die early during embryogenesis [19,20], indicating that the CTR1 protein is crucial for normal development. However, the biochemistry and cell biology of mammalian CTR1 has not yet been examined. This study on the hCTR1 protein represents the initial characterization of biosynthesis and post-translational processing of hCTR1, and its subcellular localization.

In accordance with the ubiquitous mRNA expression of hCTR1 in tissue [18], we found that hCTR1 was expressed in every investigated cell line. The biosynthesis of hCTR1 was the result of extensive glycosylation of a 23-kDa core polypeptide via the formation of a 28-kDa precursor polypeptide. This precursor was further modified to a 35-kDa mature protein within 60 min. Mature hCTR1 differed in size between the investigated cell lines and appeared as heterogeneous smears on SDS/PAGE, which is also indicative of the presence of oligosaccharide chains. Although the same glycosylation machinery is available to all proteins that enter the secretory pathway in a given cell, it is possible that proteins emerge with characteristic glycosylation patterns and heterogeneous populations of glycans at each glycosylation site [35]. In the presence of tunicamycin the mature hCTR1 protein was not formed; however, in addition to a polypeptide of 23 kDa, also a polypeptide of 30 kDa was detected. The 30-kDa polypeptide was most likely the result of O-linked glycosylation of the precursor lacking N-linked oligosaccharides, since O-linked glycosylation is not inhibited by tunicamycin treatment [36]. After 2 h of pulse chase, approximately equal amounts of 23-kDa core protein and partially glycosylated 30-kDa protein were detected by anti-hCTR1 antibody, whereas in the absence of tunicamycin most of the newly synthesized hCTR1 was converted to the mature form. An explanation that may account for this delay in processing is the fact that newly synthesized proteins, which are incompletely glycosylated, folded or assembled, are retained in the endoplasmic reticulum and eventually degraded via the quality-control system [37]. In conclusion, the human CTR1 protein is heavily glycosylated similarly to the yeast Ctr1 protein, which is also extensively modified by the addition of O-linked oligosaccharides [28]; the

role of these oligosaccharides in copper transport and intracellular sorting is the subject of further study.

The 35-kDa protein detected by the anti-hCTR1 antibody was not sensitive to Endo-H treatment, suggesting a late- or post-Golgi localization of this protein. Endo H is widely used to distinguish complex oligosaccharides from high-mannose oligosaccharides, which are formed by post-translational modification during their passage through the Golgi apparatus [38]. In immunofluorescence studies, we found that intracellular hCTR1 localization was dependent on the cell type. In HeLa cells amongst others, hCTR1 was predominantly localized in a perinuclear vesicular compartment. Plasma membrane localization was not observed in these cells, but we do not exclude cell surface expression below detection limits. Intracellular hCTR1 partially co-localized with the Golgi markers p230 and p58 [39,40] and was insensitive to redistribution by BFA, but sensitive to nocodazole treatment. Resident proteins of the *cis*-, medial- and *trans*-Golgi cisternae return to the endoplasmic retuculum upon BFA treatment [41,42], whereas the destination of proteins of the TGN is not known. Several studies indicate that these proteins of the TGN are insensitive to BFA treatment [43–45], whereas others support the hypothesis that the TGN proteins are BFA-sensitive [46–48]. Nocodazole treatment, by depolymerizing microtubules, results in the rapid redistribution of *trans*-Golgi and TGN proteins [49,50]. We conclude that hCTR1 is predominantly localized within the TGN or in a vesicular compartment in close apposition to the TGN in HeLa, H441, A549 and HepG2 cells under normal conditions. However, given the limitations in the resolution of immunofluorescence microscopy, further studies using immuno-electron microscopy are required to unequivocally determine the intracellular localization of hCTR1 in these cells. In a number of other cell lines, hCTR1 was abundantly detected on the cell surface under normal conditions. Taken together, cell surface localization of hCTR1 is dependent on the cell type.

These findings have important implications for the mechanisms of cellular copper import and will direct our subsequent research efforts. As a first hypothesis emanating from this work, intracellular hCTR1 could represent a pool of molecules that can be quickly recruited to the plasma membrane, as has been described for the insulin-regulated glucose transporter Glut4 [51]. Thus, we considered the possibility that hCTR1 is only localized at the cell surface in times of copper shortage, thereby providing a protective post-translational mechanism against excess copper import. In accordance with this hypothesis, the yeast Ctr1 protein is constitutively expressed on the cell surface, but rapidly endocytosed upon high copper concentration in the medium [52]. However, in the present study we show clearly that hCTR1 localization was not dependent on copper availability in HeLa and Caco2 cells. Secondly, we speculate that intracellular hCTR1 could in fact actively participate in cellular copper import. Other metal transporters, including the ATP7A and ATP7B proteins, as well as DMT1/NRAMP2, are also localized and, presumably, functioning in intracellular organelles [25,30,53]. This model would require copper to be endocytosed and delivered to the hCTR1 resident compartment. Alternatively, hCTR1 may rapidly cycle between the perinuclear intracellular compartment and the plasma membrane, where it binds the metal, leading to endocytosis of the hCTR1–copper complex and subsequent import of copper into the cytoplasm. This mechanism would resemble the uptake of transferrin-bound iron by the TFR [34]. In line with this suggestion, inhibition of endocytosis in HeLa cells resulted in a marked redistribution of hCTR1 to a more diffuse cellular compartment. Importantly, hCTR1 was also clearly located on the cell surface under these conditions, comparable with the TFR. Thus, these results suggest that the steady-state localization of hCTR1 is the result of a dynamic process, which involves constitutive endocytosis of the protein from the plasma membrane.

Previous cell biological studies on the copper export pumps mutated in Menkes disease and Wilson disease, ATP7A and ATP7B, revealed that the intracellular localization of these proteins is dependent on the copper concentration [25,29–32]. These results [25,29–32] indicated that a critical step in mammalian copper homoeostasis is exerted by control of cellular copper efflux. Our results suggest an additional cell-specific control of copper uptake, which involves the localization of the hCTR1 protein. Whereas the importance of CTR1 for normal development has recently been established in mice [19,20], further studies are required to completely comprehend the mechanisms that determine CTR1 localization.

We are grateful to E. Bouwens for technical assistance, Dr J. Fransen and Dr J. D. Gitlin for gifts of antibodies, Dr G. Posthuma for help with confocal microscopy, Dr G. J. Strous for valuable discussions, and S. van Mil for critical evaluation of this manuscript. This work was supported by grant 902-23-252 from the Dutch Organization for Scientific Research (NWO) and by the Wilhelmina Research Foundation (to L. W. J. K.).

REFERENCES

1 Danks, D. M. (1989) Disorders of copper transport. In The Metabolic Basis of Inherited Disease (Scriver, C. R., Beaudet, A. L., Sly, W. S. and Valle, D., eds.), pp. 1411–1432, McGraw–Hill, New York
2 Vulpe, C. D. and Packman, S. (1995) Cellular copper transport. Annu. Rev. Nutr. **15**, 293–322
3 Fridovich, I. (1978) The biology of oxygen radicals. Science (Washington, D.C.) **201**, 875–880
4 Halliwell, B. (1991) Reactive oxygen species in living systems: source, biochemistry, and role in human disease. Am. J. Med. **91**, 14S–22S
5 Bull, P. C. and Cox, D. W. (1994) Wilson disease and Menkes disease: new handles on heavy-metal transport. Trends Genet. **10**, 246–252
6 Bull, P. C., Thomas, G. R., Rommens, J. M., Forbes, J. R. and Cox, D. W. (1993) The Wilson disease gene is a putative copper transporting P-type ATPase similar to the Menkes gene. Nat. Genet. **5**, 327–337
7 Chelly, J., Tumer, Z., Tonnesen, T., Petterson, A., Ishikawa-Brush, Y., Tommerup, N., Horn, N. and Monaco, A. P. (1993) Isolation of a candidate gene for Menkes disease that encodes a potential heavy metal binding protein. Nat. Genet. **3**, 14–19
8 Mercer, J. F., Livingston, J., Hall, B., Paynter, J. A., Begy, C., Chandrasekharappa, S., Lockhart, P., Grimes, A., Bhave, M., Siemieniak, D. et al. (1993) Isolation of a partial candidate gene for Menkes disease by positional cloning. Nat. Genet. **3**, 20–25
9 Vulpe, C., Levinson, B., Whitney, S., Packman, S. and Gitschier, J. (1993) Isolation of a candidate gene for Menkes disease and evidence that it encodes a copper-transporting ATPase. Nat. Genet. **3**, 7–13
10 Yamaguchi, Y., Heiny, M. E. and Gitlin, J. D. (1993) Isolation and characterization of a human liver cDNA as a candidate gene for Wilson disease. Biochem. Biophys. Res. Commun. **197**, 271–277
11 Dancis, A., Yuan, D. S., Haile, D., Askwith, C., Eide, D., Moehle, C., Kaplan, J. and Klausner, R. D. (1994) Molecular characterization of a copper transport protein in *S. cerevisiae:* an unexpected role for copper in iron transport. Cell (Cambridge, Mass.) **76**, 393–402
12 Knight, S. A., Labbe, S., Kwon, L. F., Kosman, D. J. and Thiele, D. J. (1996) A widespread transposable element masks expression of a yeast copper transport gene. Genes Dev. **10**, 1917–1929
13 Lin, S.-J., Pufahl, R. A., Dancis, A., O'Halloran, T. V. and Culotta, V. C. (1997) A role for the *Saccharomyces cerevisiae* ATX1 gene in copper trafficking and iron transport. J. Biol. Chem. **272**, 9215–9220
14 Culotta, V. C., Klomp, L. W. J., Strain, J., Casareno, R. L. B., Krems, B. and Gitlin, J. D. (1997) The copper chaperone for superoxide dismutase. J. Biol. Chem. **272**, 23469–23472
15 Glerum, D. M., Shtanko, A. and Tzagoloff, A. (1996) Characterization of COX17, a yeast gene involved in copper metabolism and assembly of cytochrome oxidase. J. Biol. Chem. **271**, 14504–14509
16 Klomp, L. W. J., Lin, S.-J., Yuan, D. S., Klausner, R. D., Culotta, V. C. and Gitlin, J. D. (1997) Identification and functional expression of HAH1, a novel human gene involved in copper homeostasis. J. Biol. Chem. **272**, 9221–9226

17 Amaravadi, R., Glerum, D. M. and Tzagoloff, A. (1997) Isolation of a cDNA encoding the human homolog of COX17, a yeast gene essential for mitochondrial copper recruitment. Hum. Genet. **99**, 329–333

18 Zhou, B. and Gitschier, J. (1997) hCTR1: a human gene for copper uptake identified by complementation in yeast. Proc. Natl. Acad. Sci. U.S.A. **94**, 7481–7486

19 Kuo, Y. M., Zhou, B., Cosco, D. and Gitschier, J. (2001) The copper transporter CTR1 provides an essential function in mammalian embryonic development. Proc. Natl. Acad. Sci. U.S.A. **98**, 6836–6841

20 Lee, J., Prohaska, J. R. and Thiele, D. J. (2001) Essential role for mammalian copper transporter Ctr1 in copper homeostasis and embryonic development. Proc. Natl. Acad. Sci. U.S.A. **98**, 6842–6847

21 Lee, J., Prohaska, J. R., Dagenais, S. L., Glover, T. W. and Thiele, D. J. (2000) Isolation of a murine copper transporter gene, tissue specific expression and functional complementation of a yeast copper transport mutant. Gene **254**, 87–96

22 Møller, L. B., Petersen, C., Lund, C. and Horn, N. (2000) Characterization of the *hCTR1* gene: genomic organization, functional expression, and identification of a highly homologous processed gene. Gene **257**, 13–22

23 Kreis, T. E. (1986) Microinjected antibodies against the cytoplasmic domain of vesicular stomatitis virus glycoprotein block its transport to the cell surface. EMBO J. **5**, 931–941

24 Laemmli, U. K. (1970) Cleavage of structural proteins during the assembly of the head of bacteriophage T4. Nature (London) **227**, 680–685

25 Yamaguchi, Y., Heiny, M. E., Suzuki, M. and Gitlin, J. D. (1996) Biochemical characterization and intracellular localization of the Menkes disease protein. Proc. Natl. Acad. Sci. U.S.A. **93**, 14030–14035

26 Kuo, S. C. and Lampen, O. (1976) Tunicamycin inhibition of [^{3}H]glucosamine incorporation into yeast glycoproteins: binding of tunicamycin and interaction with phospholipids. Arch. Biochem. Biophys. **172**, 574–581

27 Tarentino, A. L. and Maley, F. (1974) Purification and properties of an endo-β-*N*-acetylglucosaminidase from hen oviduct. J. Biol. Chem. **249**, 811–817

28 Dancis, A., Haile, D., Yuan, D. S. and Klausner, R. D. (1994) The *Saccharomyces cerevisiae* copper transport protein (Ctr1p). Biochemical characterization, regulation by copper, and physiologic role in copper uptake. J. Biol. Chem. **269**, 25660–25667

29 Petris, M. J., Mercer, J. F., Culvenor, J. G., Lockhart, P., Gleeson, P. A. and Camakaris, J. (1996) Ligand-regulated transport of the Menkes copper P-type ATPase efflux pump from the Golgi apparatus to the plasma membrane: a novel mechanism of regulated trafficking. EMBO J. **15**, 6084–6095

30 Hung, I. H., Suzuki, M., Yamaguchi, Y., Yuan, D. S., Klausner, R. D. and Gitlin, J. D. (1997) Biochemical characterization of the Wilson disease protein and functional expression in the yeast *Saccharomyces cerevisiae*. J. Biol. Chem. **272**, 21461–21466

31 Payne, A. S. and Gitlin, J. D. (1998) Functional expression of the Menkes disease protein reveals common biochemical mechanisms among the copper-transporting P-type ATPases. J. Biol. Chem. **273**, 2765–2770

32 Roelofsen, H., Wolters, H., Van Luyn, M. J., Miura, N., Kuipers, F. and Vonk, R. J. (2000) Copper-induced apical trafficking of ATP7B in polarized hepatoma cells provides a mechanism for biliary copper excretion. Gastroenterology **119**, 782–793

33 Yancey, P. G., Rodrigueza, W. V., Kilsdonk, E. P., Stoudt, G. W., Johnson, W. J., Phillips, M. C. and Rothblat, G. H. (1996) Cellular cholesterol efflux mediated by cyclodextrins. Demonstration of kinetic pools and mechanism of efflux. J. Biol. Chem. **271**, 16026–16034

34 Ciechanover, A., Schwartz, A. L. and Lodish, H. F. (1983) Sorting and recycling of cell surface receptors and endocytosed ligands: the asialoglycoprotein and transferrin receptors. J. Cell. Biochem. **23**, 107–130

35 Rudd, P. M. and Dwek, R. A. (1997) Glycosylation: heterogeneity and the 3D structure of proteins. Crit. Rev. Biochem. Mol. Biol. **6**, 1–100

36 Orlean, P., Kuranda, M. J. and Albright, C. F. (1991) Analysis of glycoproteins from *Saccharomyces cerevisiae*. Methods Enzymol. **194**, 682–697

37 Hammond, C. and Helenius, A. (1995) Quality control in the secretory pathway. Curr. Opin. Cell. Biol. **7**, 523–529

38 Ronin, C., Stannard, B. S., Rosenbloom, I. L., Magner, J. A. and Weintraub, B. D. (1984) Glycosylation and processing of high-mannose oligosaccharides of thyroid-stimulating hormone subunits: comparison to nonsecretory cell glycoproteins. Biochemistry **23**, 4503–4510

39 Erlich, R., Gleeson, P. A., Campbell, P., Dietzsch, E. and Toh, B. H. (1996) Molecular characterization of trans-Golgi p230. A human peripheral membrane protein encoded by a gene on chromosome 6p12-22 contains extensive coiled-coil α-helical domains and a granin motif. J. Biol. Chem. **271**, 8328–8337

40 Lahtinen, U., Hellman, U., Wernstedt, C., Saraste, J. and Pettersson, R. F. (1996) Molecular cloning and expression of a 58-kDa cis-Golgi and intermediate compartment protein. J. Biol. Chem. **271**, 4031–4037

41 Lippincott-Schwartz, J., Yuan, L. C., Bonifacino, J. S. and Klausner, R. D. (1989) Rapid redistribution of Golgi proteins into the ER in cells treated with brefeldin A: evidence for membrane cycling from Golgi to ER. Cell (Cambridge, Mass.) **56**, 801–813

42 Klausner, R. D., Donaldson, J. G. and Lippincott-Schwartz, J. (1992) Brefeldin A: insights into the control of membrane traffic and organelle structure. J. Cell Biol. **116**, 1071–1080

43 Chege, N. W. and Pfeffer, S. R. (1990) Compartmentation of the Golgi complex: brefeldin-A distinguishes trans-Golgi cisternae from the trans-Golgi network. J. Cell. Biol. **111**, 893–899

44 Strous, G. J., van Kerkhof, P., van Meer, G., Rijnboutt, S. and Stoorvogel, W. (1993) Differential effects of brefeldin A on transport of secretory and lysosomal proteins. J. Biol. Chem. **268**, 2341–2347

45 Horn, M. and Banting, G. (1994) Okadaic acid treatment leads to a fragmentation of the trans-Golgi network and an increase in expression of TGN38 at the cell surface. Biochem. J. **301**, 69–73

46 Bose, S., Chapin, S. J., Seetharam, S., Feix, J., Mostov, K. E. and Seetharam, B. (1998) Brefeldin A (BFA) inhibits basolateral membrane (BLM) delivery and dimerization of transcobalamin II receptor in human intestinal epithelial Caco-2 cells. BFA effects on BLM cholesterol. J. Biol. Chem. **273**, 16163–16169

47 Ladinsky, M. S. and Howell, K. E. (1992) The trans-Golgi network can be dissected structurally and functionally from the cisternae of the Golgi complex by brefeldin A. Eur. J. Cell Biol. **59**, 92–105

48 Cid-Arregui, A., Parton, R. G., Simons, K. and Dotti, C. G. (1995) Nocodazole-dependent transport, and brefeldin A-sensitive processing and sorting, of newly synthesized membrane proteins in cultured neurons. J. Neurosci. **15**, 4259–4269

49 De Brabander, M. J., Van de Veire, R. M., Aerts, F. E., Borgers, M. and Janssen, P. A. (1976) The effects of methyl [5-(2-thienylcarbonyl)-1H-benzimidazol-2-yl] carbamate, (R 17934; NSC 238159), a new synthetic antitumoral drug interfering with microtubules, on mammalian cells cultured *in vitro*. Cancer Res. **36**, 905–916

50 Yang, W. and Storrie, B. (1998) Scattered Golgi elements during microtubule disruption are initially enriched in trans-Golgi proteins. Mol. Biol. Cell **9**, 191–207

51 James, D. E., Strube, M. and Mueckler, M. (1989) Molecular cloning and characterization of an insulin-regulatable glucose transporter. Nature (London) **338**, 83–87

52 Ooi, C. E., Rabinovich, E., Dancis, A., Bonifacino, J. S. and Klausner, R. D. (1996) Copper-dependent degradation of the *Saccharomyces cerevisiae* plasma membrane copper transporter Ctr1p in the apparent absence of endocytosis. EMBO J. **15**, 3515–3523

53 Tabuchi, M., Yoshimori, T., Yamaguchi, K., Yoshida, T. and Kishi, F. (2000) Human NRAMP2/DMT1, which mediates iron transport across endosomal membranes, is localized to late endosomes and lysosomes in HEp-2 cells. J. Biol. Chem. **275**, 22220–22228

Received 8 December 2001/31 January 2002; accepted 25 March 2002